The Silicon Vertex Detector of the Belle II Experiment

J. Wiechczynski,[r,*] **K. Adamczyk,**[r] **H. Aihara,**[p] **S. Bacher,**[r] **S. Bahinipati,**[e]

J. Baudot,[d] **P. K. Behera,**[f] **S. Bettarini,**[j,k] **T. Bilka,**[b] **A. Bozek,**[r] **F. Buchsteiner,**[a]

G. Casarosa,[j,k] **L. Corona,**[k] **S. B. Das,**[g] **G. Dujany,**[d] **C. Finck,**[d] **F. Forti,**[j,k]

M. Friedl,[a] **A. Gabrielli,**[l,m] **B. Gobbo,**[m] **S. Halder,**[i] **K. Hara,**[q,n] **S. Hazra,**[i]

T. Higuchi,[o] **C. Irmler,**[a] **A. Ishikawa,**[q,n] **Y. Jin,**[m] **M. Kaleta,**[r] **A. B. Kaliyar,**[a]

J. Kandra,[b] **K. H. Kang,**[o] **P. Kodyš,**[b] **T. Kohriki,**[q] **R. Kumar,**[h] **K. Lalwani,**[g]

K. Lautenbach,[c] **R. Leboucher,**[c] **J. Libby,**[f] **L. Martel,**[d] **L. Massaccesi,**[j,k]

G. B. Mohanty,[i] **S. Mondal,**[j,k] **K. R. Nakamura,**[q,n] **Z. Natkaniec,**[r] **Y. Onuki,**[p]

F. Otani,[o] **A. Paladino**[A,j,k] **E. Paoloni,**[j,k] **K. K. Rao,**[i] **I. Ripp-Baudot,**[d] **G. Rizzo,**[j,k]

Y. Sato,[q] **C. Schwanda,**[a] **J. Serrano,**[c] **T. Shimasaki,**[o] **J. Suzuki,**[q] **S. Tanaka,**[q,n]

F. Tenchini,[j,k] **R. Thalmeier,**[a] **R. Tiwary,**[i] **T. Tsuboyama,**[q] **Y. Uematsu,**[p] **L. Vitale,**[l,m]

Z. Wang,[p] **H. Yin,**[a] **L. Zani**[B,c] **and F. Zeng**[o] **(Belle-II SVD collaboration)**

[a]*Institute of High Energy Physics, Austrian Academy of Sciences, 1050 Vienna, Austria*

[b]*Faculty of Mathematics and Physics, Charles University, 121 16 Prague, Czech Republic*

[c]*Aix Marseille Université , CNRS/IN2P3, CPPM, 13288 Marseille, France,* [B]*presently at INFN Sezione di Roma Tre, I-00185 Roma, Italy*

[d]*IPHC, UMR 7178, Université de Strasbourg, CNRS, 67037 Strasbourg, France*

[e]*Indian Institute of Technology Bhubaneswar, Bhubaneswar 752050, India*

[f]*Indian Institute of Technology Madras, Chennai 600036, India*

[g]*Malaviya National Institute of Technology Jaipur, Jaipur 302017, India*

[h]*Punjab Agricultural University, Ludhiana 141004, India*

[i]*Tata Institute of Fundamental Research, Mumbai 400005, India*

[j]*Dipartimento di Fisica, Università di Pisa, I-56127 Pisa, Italy,* [A]*presently at INFN Sezione di Bologna, I-40127 Bologna, Italy*

[k]*INFN Sezione di Pisa, I-56127 Pisa, Italy*

[l]*Dipartimento di Fisica, Università di Trieste, I-34127 Trieste, Italy*

[m]*INFN Sezione di Trieste, I-34127 Trieste, Italy*

[n]*The Graduate University for Advanced Studies (SOKENDAI), Hayama 240-0193, Japan*

[o]*Kavli Institute for the Physics and Mathematics of the Universe, University of Tokyo, Kashiwa 277-8583, Japan*

[p]*Department of Physics, University of Tokyo, Tokyo 113-0033, Japan*

[q]*High Energy Accelerator Research Organization (KEK), Tsukuba 305-0801, Japan*

[r]*H. Niewodniczanski Institute of Nuclear Physics, Krakow 31-342, Poland*

E-mail: wiechczynski@belle2.ifj.edu.pl

---

*Speaker

The Belle II experiment operating at the asymmetric-energy e^+e^- SuperKEKB collider, located in Tsukuba (Japan), has been collecting data since March 2019. Its excellent vertexing abilities are provided by the vertex detector, part of which is the silicon-strip vertex detector (SVD) that plays a crucial role in the charged-particle tracking close to the interaction point. The SVD has operated successfully and efficiently over the whole period of data taking so far. In this article, we briefly discuss its purpose, structure and basic description of the front-end electronics. The main quantities related to the SVD performance are presented. The foreseen increase in SuperKEKB luminosity will lead to higher background, so we describe its impact on the SVD performance. A quick overview of the radiation damage campaign is presented to show the predicted behaviour of the sensors subjected to high radiation, whose level is constantly monitored. We also discuss the ongoing software development to account for the high occupancy expected in the future. In particular, the utilization of the SVD hit time information is presented as a very important quantity to suppress off-time background hits and tracks. Finally, the work done during the first long shutdown of SuperKEKB is briefly described, during which a major upgrade of the pixel detector has been successfully done. Resumption of the beam operation is expected in early 2024.

Keywords: Silicon strip detector, Vertex detector, Tracking detector, Belle II

1. Introduction

The Belle II [1] experiment is dedicated to search for physics beyond the standard model at the intensity frontier. It operates at the SuperKEKB collider located at KEK, Tsukuba in Japan, providing asymmetric beams of 7 GeV electrons and 4 GeV positrons. In the accelerator's default operation regime, the center-of-mass energy is set to the $\Upsilon(4S)$ resonance, hence it produces a huge sample of B mesons via the $e^+e^- \rightarrow \Upsilon(4S) \rightarrow B\bar{B}$ process. So far, SuperKEKB achieved the highest instantaneous luminosity of 4.7×10^{34} cm^{-2}s^{-1}, which is the current world record. The Belle II detector is a multipurpose spectrometer characterized by excellent vertexing capability and good hermeticity, which has accumulated 424 fb^{-1} to date, and its final goal is to collect a data sample of 50 ab^{-1}, that will be possible with a constant increase of the SuperKEKB instantaneous luminosity up to our final goal of 6×10^{35} cm^{-2}s^{-1}.

Belle II is composed of various sub-detectors with the vertex detector (VXD) being the closest to the interaction point. It is divided into two further subsystems. The innermost part is the pixel detector (PXD), which is based on depleted field effect transistor pixel sensors. The PXD consists of two layers (numbered 1-2) and its main goal is the precise determination of the decay vertices. Outside the PXD is the silicon-strip vertex detector (SVD) [2] with four layers (numbered 3-6) that mostly extrapolates the measured tracks to the PXD, defining the so-called region of interest (ROI), which significantly reduces the amount of data recorded by the PXD. The SVD also performs standalone tracking for low-momentum charged particles and contributes to their identification by providing energy loss information.

2. SVD structure

Each SVD layer is composed of a number of double-sided silicon strip detectors (DSSDs) that are manufactured on an n-type bulk wafer with a thickness of about 300 μm (Figure 1). One side of the sensor is covered by the p-type silicon strips placed in parallel to the beam axis that determine the $r - \phi$ coordinates (distance from the z-axis and azimuthal angle, respectively), and the n-type strips are placed perpendicularly on the other side of the bulk, measuring the z coordinate (collinear to the electron beam). Figure 1 (left) shows a schematic picture of SVD layers and associated sensors with increasing numbering from the forward (FWD) to the backward (BWD) regions. Such structure is repeated along the azimuthal direction forming different ladders and the so-called windmill geometry of the SVD. The sensors differ depending on the layer and the region in which they are placed in the SVD. In the FWD part, for layers 4-6, they have a trapezoidal shape
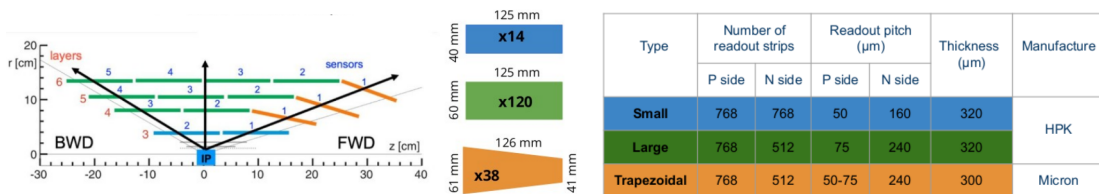

Type	Number of readout strips		Readout pitch (μm)		Thickness (μm)	Manufacture
	P side	N side	P side	N side		
Small	768	768	50	160	320	HPK
Large	768	512	75	240	320	HPK
Trapezoidal	768	512	50-75	240	300	Micron

Figure 1: *Schematic picture of SVD sensors forming different layers (left) and a table summarizing the parameters for each type of sensor (right).*

and are slanted in the region that, due to the asymmetric beams, is characterised by the highest track multiplicity. In addition, in layer 3 the sensors are smaller and contain more n-type strips than that in layers 4-6. This also implies the readout pitch (distance between two readout strips) to be much smaller for p-side strips with respect to the n-side. To improve spatial resolution, a floating strip is placed between two readout strips on both p- and n-sides. The charge induced in the floating strip is shared by the neighboring strips, reducing the effective strip pitch to half of the readout pitch. The right table of Figure 1 summarises the sensor parameters. The SVD consists of 224 thousand readout strips and 172 sensors with an active area of 1.2 m^2.

2.1 Front-end electronics

For the readout we use APV25 chips [3]. For the central part of SVD (except for layer 3), the chips are attached directly to the DSSD sensors via flex circuits bent over the DSSD edge (Origami concept). The edge sensors use hybrid boards located outside the active volume. The APV25 has 128 channels per chip and amplifiers that provide a shaping time of 50 ns. Radiation hardness exceeds 100 Mrad and the power consumption is around 0.4 W/chip. The sampling frequency is 32 MHz and after the trigger's arrival we can collect six consecutive signal samples in total with the multipeak mode. To account for higher luminosity in the future, we have introduced the so-called "3/6 mixed acquisition mode", which allows switching between three and six samples recorded on an event-by-event basis, based on the trigger type (and hence its time accuracy) for a particular event. This mode, already prepared and tested, significantly reduces the data size, which can be crucial in high background conditions.

3. SVD performance

Since the start of the operation we have observed very smooth performance of the SVD, with a very few masked strips (less than 1%). Moreover, the environment has been stable and the evolution of calibration constants is consistent with expectation. Also, the effects of radiation damage are well under control.

Several quantities related to the SVD performance - sensor efficiency, signal-to-noise ratio, and both spatial and time resolution - are constantly monitored. Regarding SVD sensor efficiency, the values for all sensors are typically over 99% and they are also very stable over the whole period of data taking. Clusters are formed from adjacent strips with significant signal and the charge collected in a given cluster strongly depends on the incident angle of the track. Over time, we observe very similar cluster charge in all the sensors once normalized to the track's length. For layer 4-5-6 on the n-type strips we observe 10-30% loss of the signal due to the large pitch combined with the presence of a floating strip. Another important quantity is the signal-to-noise ratio (SNR), which is satisfactory for all 172 sensors. The SNR MPV is ranging from 13 to 30, depending on the sensor position, due to the track incident angle with the sensor, and on the sensor side, with smaller SNR for the p-sides, due to larger noise for the longer strip length. A small decrease of cluster SNR value is observed in 2022 measurement, due to increased noise from radiation damage by approximately 20%– 30%. In Figure 2 the distributions of cluster charge (left) and SNR (right) are presented, where histograms representing the data collected in 2020 and 2022 are superimposed.
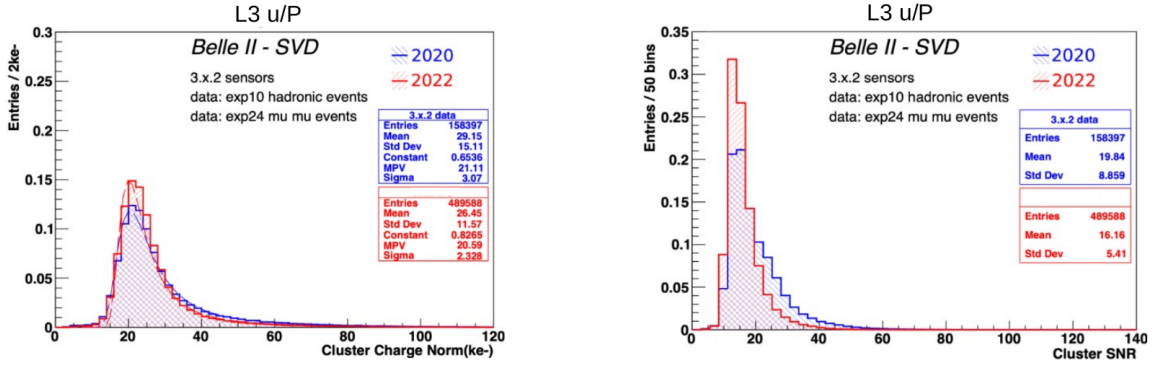
Figure 2: *Distribution of cluster charge (left) and signal-to-noise ratio (right) for layer 3 (p-side). Comparison between data taken in 2020 (blue) and 2022 (red) is presented.*

Both position and time resolution are very important metrics for excellent SVD performance. The position resolution measurement is based on the residuals, i.e., the clusters' positions with respect to the intercept of the unbiased tracks' extrapolation, and it is evaluated with a large sample of $e^+e^- \to \mu^+\mu^-$ decays. As shown in Figure 3, this quantity depends on the incident angle and is very stable during the period of the Belle II operation. Cluster position is calculated as the center of gravity (i.e. weighted mean) of the various strip positions inside the cluster, using the collected charge as strip weight. The cluster position resolution then depends on cluster size and on the strip signal-to-noise ratio, varying with the track incident angle with an expected non monotone dependence visible in Figure 3. For zero incident angle, with perpedicular tracks more likely to produce a single strip cluster, one can only achieve a "digital" resolution, corresponding to the standard deviation of a flat distribution inside implanted strip pitch (floating strip pitch/$\sqrt{12}$). The resolution improves with more than one strip in the cluster, adding the the center of gravity analog information. It reaches a minimum for two strip clusters, corresponding to the incident angle for which the projection of the track along the direction perpendicular to the strips on the detector plane is two floating strip pitches (4 and 14 degrees for the layer 3 p- and n-sides pitches). For large incident angle, since the signal collected in each strip decreases with the incident angle θ (proportional to pitch/$\sin(\theta)$), the consequent reduction of the strip signal-to-noise ratio degrades the cluster position resolution, visible in Figure 3. In general, the resolution for the n-side (left plot) is about two times worse with respect to that for the u-side, which is a result of the different pitch and strip signal-to-noise ratio on the two sides.

Hit time resolution is measured with respect to the event time of the collision provided by central drift chamber (CDC) and exhibits a very good resolution of less than 3 ns for the clusters associated to tracks. Using the average value of all the hits on a given track, the so-called "track-time" can be computed, slightly improving the time resolution. Furthermore, the "event-time" can be determined using all the clusters associated to selected tracks in an event. In such a way, the "event time" can be computed by the SVD with a resolution of the order of 1 ns, while the computation is around 2000 times faster than the one based on CDC. This feature will be especially important in the higher luminosity environment, as it can significantly speed up the reconstruction process at the high-level trigger.
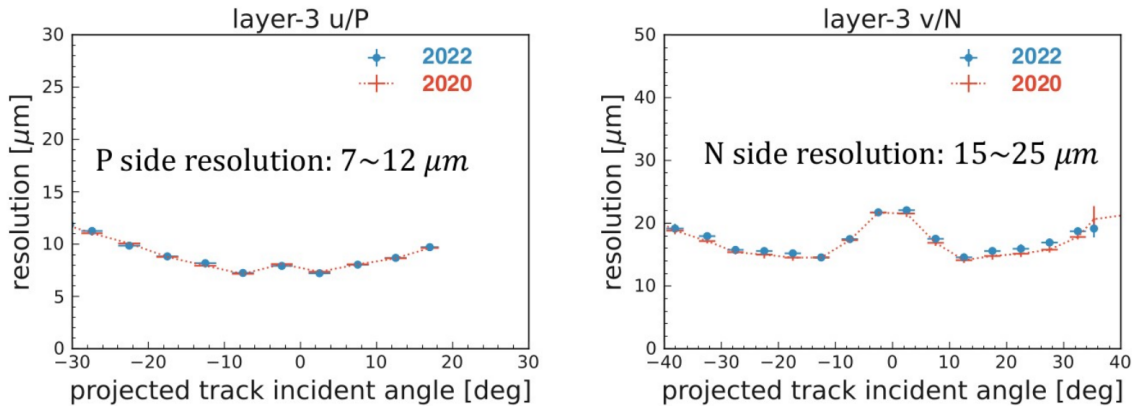
Figure 3: *Distributions of position resolution for p-side (left) and n-side (right) as a function of the track incident angle. A comparison between data taken in 2020 (dots) and 2022 (dotted lines) is presented.*
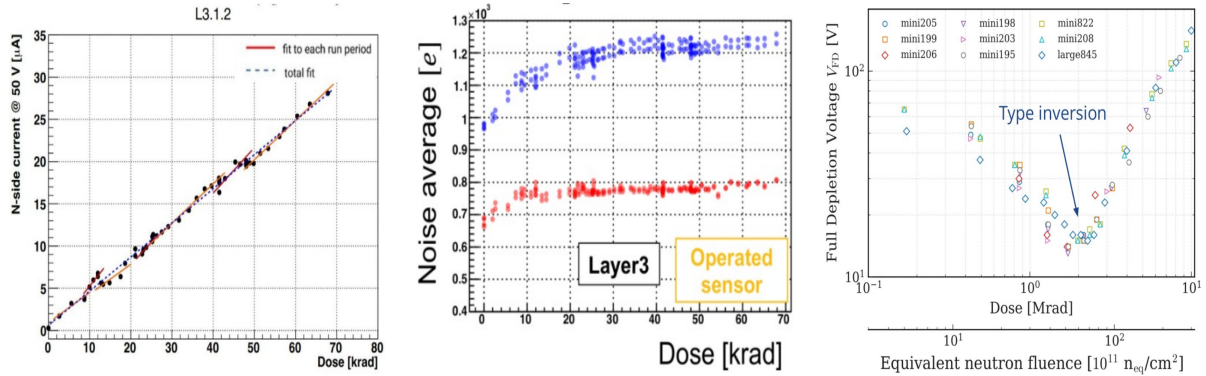

Figure 4: *Left plot: Leakage current as a function of the accumulated dose; Center plot: the average noise level as a function of the accumulated dose for the p-side (blue dots) and n-side (red dots); Right plot: full depletion voltage as a function of the accumulated dose with the type inversion observed at 2 Mrad.*

4. Radiation effects

In the high-energy physics experiments, the effects from radiation damage coming from machine related background is a major factor that degrades the sensor performance with time. The SVD accumulated dose is constantly measured using data from diamond sensors that are mounted on the IP beam pipe, and the corresponding level of the equivalent neutron fluence is evaluated using the ratio of equivalent neutron fluence to dose estimated from Monte Carlo simulation. Several effects related to radiation damage must be taken into account. A linear increase of the leakage current as a function of radiation damage is observed in the sensors, as expected from the bulk damage described by the NIEL model [4], and shown in Figure 4 left. The sensor current is shown as a function of the accumulated dose for one of the layer 3 sensors most exposed, that received about 70 krad to date, corresponding to an equivalent neutron fluence of about 1.6×10^{11} n_{eq}/cm^2. So far, this increase has had a negligible contribution to the noise because of both the small leakage

current and the short APV25 shaping time. The rate of the leakage current increase measured is consistent with the experience from other experiments working with similar detectors and in comparable conditions [5]. However, we expect some significant impact on the strip noise due to the sensor leakage current, and hence a deterioration in SNR, for the dose of ~6 Mrad, which is considered as SVD dose limit to preserve optimal performance. The strip noise for unirradiated modules is dominated by the interstrip capacitance. During the operation we have observed an increase in its value of about 20% (30%) for n-side (p-side), due to effects of surface radiation damage that increases the interstrip capacitance, but it is expected to saturate, as also visible in Figure 4 center.

Another relevant effect of the bulk radiation damage is the impact on depletion voltage. The expected future radiation levels at the nominal luminosity, of about 0.35 Mrad/year and 8×10^{11} n_{eq}/cm^2/year, are affected by large uncertainty due to the machine evolution as well as a possible redesign of the interaction region. To better explore the possible effects of bulk damage in the SVD sensors after bulk type inversion, an irradiation campaign was conducted in July 2022 at ELPH, Tohoku University. Several SVD sensors have been exposed to a 90 MeV electrons beam, up to 10 Mrad, corresponding to an equivalent neutron fluence of 3×10^{13} n_{eq}/cm^2. The decrease of the depletion voltage has been observed up to the point of bulk type inversion, which occurred at 2 Mrad ($\sim 6 \times 10^{12}$ n_{eq}/cm^2), after which the depletion voltage started to increase again (Figure 4 right). Detailed measurements, whose results will be shortly published, confirmed that the sensors will still work fine after the type inversion, which meets our expectation for these types of silicon detectors. Since the beginning of the detector operation, we have not observed any change in the depletion voltage in the sensors installed in the SVD, as expected due to the small accumulated equivalent neutron fluence so far, below 2×10^{11} n_{eq}/cm^2. Considering all these results, the dose limit of 6 Mrad and the extrapolation of the background levels quoted above, the SVD has a wide safety margin for the accumulated radiation damage even after 10 years of the operation at the target luminosity.

5. High background scenario and related software/hardware developments

With the increase of the luminosity and the expected larger machine related background, the SVD occupancy will also increase and a deterioration of the tracking performance is expected above certain levels. So far, the average hit occupancy is 0.5% for layer 3, which does not degrade the performance. Nonetheless, the background extrapolation for different future scenarios has been performed with detailed simulations of the various contributions (beam-gas, Toushek, etc.) and applying appropriate data-simulation scale factors [6]. These studies predict that for the nominal luminosity we can reach an occupancy in layer 3 very close to the limit of 4.7%, above which the tracking performance deteriorates. These predictions have large uncertainties coming from poorly known machine evolution in the future, with a possible redesign of the interaction region. In the most conservative scenario, the layer-3 occupancy can increase up to ~8.7%, which is far beyond the modest tracking performance. Such a scenario motivates us to develop the SVD reconstruction software, as well as to seriously consider the VXD upgrade [7], since the safety factor might be too small to ensure good quality data. The technology assessment related to this hardware upgrade is currently ongoing.

An important effort related to the software development is the utilization of the hit time information from the SVD. The real signal hits come from well-triggered collisions, but the SVD acquisition window (~ 100 ns) is much wider with respect to the SuperKEKB bunch spacing (6 ns). Therefore, we need to cope with many off-time hits related to the beam-induced background or background from the other bunches. The current selection is based on two requirements: a) time difference between p- and n-side cluster, $|t_p - t_n| < 20$ ns, and b) the absolute value of the cluster time, $|t_{p,n}| < 50$ ns. These criteria reject the majority of the background hits retaining above 99% of the signal, and based on them the SVD occupancy limit for layer 3 can be set at 4.7%. Recently, a more effective background suppression method has been developed in the form of so-called "SVD grouping". It is based on an event-by-event classification of the clusters by their time, so the clusters belonging to tracks from the same collisions are collected in the same group. Clusters from the different collisions or beam background will be placed in the other groups; finally, only the clusters belonging to the priority group will be used for the tracking. This feature reduces the fake rate (fraction of the fake tracks) by 16% for the high-background scenario. An additional fake rate reduction can be achieved by applying the selection on the track-time to reject off-time tracks. Finally, these improvements allow an increase of the SVD occupancy limit for layer 3 from 4.7% to around 6%.

6.   Activities during the Long Shutdown 1

Long shutdown 1 (LS1) started in May 2022 and one of the goals was to upgrade the VXD with a new PXD. During the first data taking period, the second layer of PXD was only partially equipped, and 5/6 of the azimuthal angle remained uncovered. The new PXD provides the full coverage, which is beneficial for more precise vertexing. Hardware activities for the VXD uninstallation and reinstallation were intense: after the VXD extraction from Belle II, the SVD was detached from the old PXD (May 16-17, 2023), then the new PXD was attached to the SVD (June 20-21, 2023) and finally the complete VXD was installed in the Belle II detector. The whole delicate procedure had neither major problems nor caused any damage. In the period of September 12 - October 1, 2023, the VXD commissioning was performed to confirm the PXD and SVD performance, and also to check the impact from the increased PXD power consumption and possible increase in the temperature on the sensor leakage current. From September 21, several cosmic runs with no magnetic field were taken to check the performance and compare them with corresponding ones for 2022 data samples. We observed no issues, in particular the noise distributions over readout channels remained basically unchanged as well as SNR for the clusters associated to the tracks, with stable excellent efficiency for all the sensors.

7.   Conclusions

To conclude, SVD has successfully operated since March 2019 with very smooth performance and without major problems. Its good vertexing quality has been confirmed by many physics measurements, in particular those related to the lifetime analyses e.g. Ref. [8]. Some radiation damage effects were observed, but without any impact on the performance so far.

However, the extrapolated background level indicates that the occupancy in the SVD can exceed the current limit that guarantees good tracking performance. Hence, several software improvements are being implemented to account for high background conditions. In particular, exploitation of the SVD hit time is of major importance. Alongside, a VXD upgrade is also under discussion to increase robustness against high background and to match a possible new interaction region.

The VXD reinstallation at Belle II with complete PXD has been successfully done during the LS1, followed by successful VXD commissioning with cosmic data. The beam operation is planned to resume in early 2024.

References

[1] T. Abe et al., Belle II Technical Design Report, arXiv:1011.0352 (2010).

[2] K. Adamczyk et al., JINST **17**, P11042 (2022).

[3] M. J. French et al., Nucl. Instrum. Meth. A **466**, 359 (2001).

[4] G. Lindstrom et al., Nucl. Instrum. Meth. A **465**, 60-69 (2000).

[5] B. Aubert et al., Nucl. Instrum. Meth. A **729**, 615 (2013).

[6] A. Natochii et al., Nucl. Instrum. Meth. A **1055**, 168550 (2023).

[7] M. Babeluk et. al., Nucl. Instrum. Meth. A **1048**, 168015 (2023).

[8] F. Abudinén et al., Phys. Rev. Lett. **130**, 071802 (2023)